GPS Solut (2010) 14:3–11
DOI 10.1007/s10291-009-0128-1

ORIGINAL ARTICLE

Phase acceleration: a new important parameter in GPS occultation technology

A. G. Pavelyev · Y. A. Liou · J. Wickert · T. Schmidt · A. A. Pavelyev

Received: 11 January 2009 / Accepted: 4 May 2009 / Published online: 31 May 2009

Abstract Based on 40 years of radio-occultation (RO) experiments, it is now recognized that the phase acceleration of radio waves (equal to the time derivative of the Doppler shift), derived from analysis of high-stability Global Positioning System (GPS) RO signals, is as important as the Doppler frequency. The phase acceleration technique allows one to convert the phase and Doppler frequency changes into refractive attenuation variations. From such derived refractive attenuation and amplitude data, one can estimate the integral absorption of radio waves. This is important for future RO missions when measuring water vapor and minor atmospheric gas constituents, because the difficulty of removing the refractive attenuation effect from the amplitude data can be avoided. The phase acceleration technique can be applied also for determining the location and inclination of sharp layered plasma structures (including sporadic E_s layers) in the ionosphere. The advantages of the phase acceleration technique are validated by analyzing RO data from the Challenging Minisatellite Payload (CHAMP) and the FORMOSA Satellite Constellation Observing Systems for Meteorology, Ionosphere, and Climate missions (FORMOSAT-3/COSMIC).

Keywords Radio occultation · Phase acceleration · Doppler frequency

A. G. Pavelyev · A. A. Pavelyev
Institute of Radio Engineering and Electronics of Russian Academy of Sciences (IRE RAS), Fryazino, Vvedenskogo sq. 1, 141190 Moscow, Russia
e-mail: pvlv@ms.ire.rssi.ru

Y. A. Liou (✉)
Center for Space and Remote Sensing Research, National Central University, Chung-Li 320, Taiwan
e-mail: yueian@csrsr.ncu.edu.tw

J. Wickert · T. Schmidt
GeoForschungsZentrum Potsdam (GFZ-Potsdam), Telegrafenberg 14473 Potsdam, Germany
e-mail: wickert@gfz-potsdam.de

Introduction

Effects of radio wave propagation are important for global real-time monitoring of the troposphere, stratosphere and ionosphere, and for estimating conditions for telecommunication in trans-atmospheric satellite-to-satellite links. The atmospheric influence introduces the phase delay (or the phase path excess relative to the phase path in free space) and Doppler shift in the carrier frequency of the radio waves. Certain physical phenomena can attenuate the intensity of radio waves by refractive spreading (the refractive attenuation effect) and atmospheric absorption losses (the integral absorption effect) as they propagate through the atmosphere. The atmospheric absorption losses at GPS frequencies are caused mainly by atmospheric oxygen (Kislyakov and Stankevich 1967). Effects of radio waves propagation are investigated during radio-occultation (RO) experiments. RO investigations of the earth's atmosphere are possible by using two satellites, one transmitting radio signals and the other receiving them. As the satellites move, the ray trajectory of radio waves passes through different portions of the atmosphere. The phase and amplitude variation profiles are recorded onboard the receiver of low earth orbital (LEO) satellites. These profiles provide information about the refractive properties of the earth's atmosphere (Kursinski et al. 1997; Yakovlev 2003;

Melbourne 2004). Initial results from RO experiments have been obtained with the use of GEOS-3/ATS-6 and Apollo/Soyuz-ATSF satellite-to-satellite tracking data (Liu 1978; Rangaswamy 1976). Problems related to RO techniques were analyzed by Kalashnikov et al. (1986). They developed general relations for changes in Doppler frequency, phase, amplitude, bending angle and absorption. Significant RO investigations began in Russia in 1990 with the use of the MIR orbital station and two geostationary satellites (Yakovlev et al. 1995). Radio links of the Ku band ($\lambda = 2$ cm) and the UHF radio band ($\lambda = 32$ cm) with transmitters of increased power and antennas with high directivity were used. The first studies proposing the usage of highly stable signals from GPS and GLONASS satellites for sounding of the atmosphere are found in Gurvich and Krasil'nikova (1987) and Yunck et al. (1988). From 1995 to 1998, the low earth orbiting satellite Microlab 1 was used to perform 11,000 measurement sessions in the L band at wavelengths of 19 and 24 cm. The vertical profiles of atmospheric temperature and electron density in the ionosphere were compared with ground-based measurements, demonstrating a high level of accuracy of the RO measurements (Ware et al. 1996; Kursinski et al. 1997; Rocken et al. 1997; Hajj et al. 2002).

The GPS RO technique is based on the assumption of global spherical symmetry of the atmosphere with a center that nearly coincides with the center of the earth. In this case, a layered structure is assumed at the ray trajectory perigee (Hajj et al. 2002). For many years, analysis of the Doppler shift variations remained the only practical way to obtain the vertical profiles of the bending angle, impact parameters and refractivity by the use of the trajectory data of satellites. In recent years, new radio-holographic techniques based on the combination of the RO amplitude and phase data have been considered, such as Fresnel diffraction theory (Marouf et al. 1986; Mortensen and Hoeg 1998), back-propagation (Gorbunov and Bengtson 1996; Hinson et al. 1997), synthetic aperture method (Lindal et al. 1987; Pavelyev 1998; Sokolovskiy 2001), radio-holographic-focused synthetic aperture (RHFSA) (Hocke et al. 1999; Igarashi et al. 2000, 2001, 2002; Pavelyev et al. 2002, 2004), canonical transform (Gorbunov and Lauritsen 2002) and the full spectrum inversion (FSI) method (Jensen et al. 2003). These studies improved the vertical resolution and accuracy in retrieving physical parameters of the atmosphere and broadened the applicability domain of the RO method. However, as described in detail by Lohman et al. (2003), there are significant difficulties in measuring the atmospheric absorption of radio waves by FSI and other radio-holographic methods based on a Fourier operator. A new and important connection among the phase acceleration, Doppler frequency and intensity variations of RO signals has been discovered by theoretical considerations and experimental analysis of radio-holograms registered during CHAMP, FORMOSAT-3 and other low orbital satellite missions (Liou and Pavelyev 2006; Pavelyev et al. 2007). This relationship gives a simple method of converting the phase acceleration (or time derivative of Doppler shift) to refractive attenuation. This is useful for estimating the integral absorption of radio waves in atmospheric communication links.

Wickert et al. (2004) showed that the amplitude channel of RO radio-holograms contains important information concerning the seasonal, geographical, and temporal distributions of the ionospheric disturbances on a global scale and indicated a possibility to estimate inclination and height of plasma layers in the lower ionosphere. The horizontal gradients of the refractivity produced by inclined plasma layers in the ionosphere can change the location of the center of spherical symmetry as shown by Wickert et al. (2004) and can cause significant variations in the amplitude and phase of RO signals. These variations sometimes were assigned without reason to the ray perigee heights of about 80 km (in which the expected contributions from the neutral gas or electron density to the RO signal evidently are negligible) (Sokolovskiy et al. 2002; Wu Dong et al. 2005). Gorbunov et al. (2002) and Sokolovskiy et al. (2002) proposed a radio-holographic back-propagation method to locate plasma irregularities in the ionosphere. A new phase acceleration technique seems to be simpler compared to the back-propagation method for determination of the height and inclination of layered plasma structures (including sporadic E_s layers) in the ionosphere (Liou and Pavelyev 2006; Pavelyev et al. 2007). In this paper, the advantages of the phase acceleration technique are described and validated by means of analysis of the CHAMP and FORMOSAT-3 RO data.

Determination of integral absorption

The geometry of the GPS radio-occultation experiment in trans-atmospheric satellite-to-satellite links is shown in Fig. 1. Point O is the center of spherical symmetry of the earth's atmosphere. The radio waves emitted by a GPS

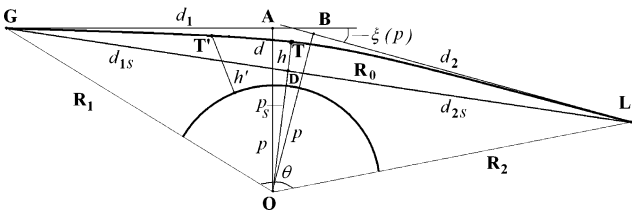

Fig. 1 Geometry of trans-atmospheric satellite-to-satellite link

satellite (point G) arrive at a receiver on board the LEO satellite (point L) along the ray trajectory GTL, where T is the ray perigee. At this point, the minimum height of the ray is h and the gradient of the refractivity $N(h)$ is perpendicular to the trajectory GTL. The projection of point T on the surface of the earth determines the geographical coordinates of the RO region. The records of the RO signal along the LEO trajectory contain the amplitudes $A_1(t)$ and $A_2(t)$, and the phase path excesses $\Phi_1(t)$ and $\Phi_2(t)$ of the radio field as functions of time for GPS transmissions at the carrier frequencies L1 and L2 ($f_1 = 1{,}574.42$ MHz and $f_1 = 1{,}227.6$ MHz). The vertical velocity of the occultation beam path is about 2 km/s. This value is many times greater than the corresponding motions of the layers in the atmosphere. Therefore, the records of the amplitude and phase at two GPS frequencies along the LEO trajectory are in essence two instantaneous 1-D radio holograms of the atmosphere, which contain important information on the spatial distribution of the physical parameters of the atmosphere. Under an assumption of the spherical symmetry, this information can be used to retrieve the vertical profile of refractivity, electron density and other important atmospheric and ionospheric parameters near the RO ray perigee point T.

Using the impact parameter p, $p = \mathrm{OB} = \mathrm{OA}$, depicted in Fig. 1, and assuming a global spherical symmetry of the atmosphere, one can express the respective relations for the phase path excess $\Phi(p)$ (the difference between the phase path in the atmosphere along the ray GTL and the same one in free space along the line of sight GDL) and the refractive attenuation $X(p)$ of radio waves as (Pavelyev et al. 2004; Liou et al. 2005).

$$\Phi(p) = L(p) + \kappa(p) - R_0 \tag{1}$$

$$X(p) = pR_0^2\left[R_1R_2d_1d_2\sin\theta\left|\frac{\partial\theta}{\partial p}\right|\right]^{-1} \tag{2}$$

$$\frac{\partial\theta}{\partial p} = \frac{1}{d_1} + \frac{1}{d_2} - \frac{\mathrm{d}\xi}{\mathrm{d}p} \tag{3}$$

$$L(p) = d_1 + d_2 + p\xi(p) \tag{4}$$

In these expressions, $L(p)$ is the distance, GABL, which consists of straight lines d_1 (GA) and d_2 (BL), and the arc AB, $\kappa(p)$ is the main refractivity part of the phase path excess, R_0, R_1 and R_2 denote the distances GDL, OG and OL, respectively. $\theta(p)$ is the central angle, and $\xi(p) = -\mathrm{d}\kappa(p)/\mathrm{d}p$ is the refractive angle (Fig. 1). The distances R_1 and R_2 are held constant in the partial differentiation $\partial\theta/\partial p$. Considering the second impact parameter p_s, $p_s = \mathrm{OD}$, relevant to the line of sight GDL (Fig. 1), and using the condition $|p–p_s| \ll p$ the first derivative of the phase path excess $\Phi(p)$ with respect to time t, giving Doppler frequency F_d, has a form

$$\frac{\mathrm{d}\Phi}{\mathrm{d}t} = F_d \approx -(p - p_s)\frac{dp_s}{dt}\left(\frac{1}{d_{1s}} + \frac{1}{d_{2s}}\right) \tag{5}$$

where d_{1s} and d_{2s} are the distances GD and DL seen in Fig. 1. As shown by Liou and Pavelyev (2006), Pavelyev et al. (2007) and Liou et al. (2007) the second derivative of the phase path excess $\Phi(p)$ can be evaluated by differentiating Eq. 5,

$$1 - X(t) = ma = m\frac{\mathrm{d}F_d}{\mathrm{d}t} = m\frac{\mathrm{d}^2\Phi(p)}{\mathrm{d}t^2} \tag{6}$$

$$m = q/\left(\frac{\mathrm{d}p_s}{\mathrm{d}t}\right)^2 \tag{7}$$

$$q = d_{1s}d_{2s}/R_0 \tag{8}$$

.

The parameter $\mathrm{d}p_s/\mathrm{d}t$ can be found from trajectory data, describing the motions of GPS and LEO satellites relative to the center of spherical symmetry, point O in Fig. 1, as follows

$$\mathrm{d}p_s/\mathrm{d}t = v + (w - v)d_{1s}/R_0 \tag{9}$$

where v and w are the respective velocity components of the GPS and LEO satellites perpendicular to the straight line GDL in the plane GOL. The components v and w are positive when pointing toward O and negative in the opposite case. Formula (6) connects the refractive attenuation $X(t)$ to the time derivative of the Doppler frequency F_d or the phase acceleration $a = \mathrm{d}F_d(t)/\mathrm{d}t = \mathrm{d}^2\Phi(p)/\mathrm{d}t^2$ via a relationship similar to classical dynamics equations. Note that the refractive attenuation $X(t)$ in Eqs. 2 and 6 depends only on the atmospheric refraction effect and ignores atmospheric absorption. Usually the parameters m and $\mathrm{d}p_s/\mathrm{d}t$ are known from orbital data because the location of the spherical symmetry center O and its projection on the line of sight, point D, are known, and the distance GD $\equiv d_{1s}$ and DL $\equiv d_{2s}$ can be easily estimated from trajectory data. Therefore, Eq. 6 gives the possibility to convert the phase acceleration a and/or Doppler frequency F_d to the refractive attenuation.

The refractive attenuation, now denoted by X_a, is determined from the amplitude data as a ratio of intensities of radio signal propagating through the atmosphere, $I_a(t)$, and free space, I_s,

$$X_a(t) = I_a(t)/I_s \tag{10}$$

The experimental value X_a is the result of the contributions from refraction and absorption effects. However, the phase acceleration in the relationship (6) depends on the refraction effect only. This provides a possibility to determine the absorption $Y(t)$ in the atmosphere as the ratio

$$Y(t) = X_a(t)/X_p(t) \quad (11)$$

with

$$X_p(t) = 1 - ma = 1 - m\frac{dF_d(t)}{dt} \quad (12)$$

where $X_p(t)$ is the refractive attenuation of radio waves recalculated from the phase data. The estimated value $X_p(t)$ contains only the contribution from refraction effects. Therefore, Eqs. 11 and 12 allow one to exclude the refractive contribution and to estimate the contribution from absorption.

Analysis of the CHAMP RO data indicates that the relationship (6) is correct. A typical example from RO session 0096 conducted on 20 November 2003 is shown in Fig. 2. The vertical profiles of the atmospheric phase path excesses measured at frequencies L1 and L2 are indicated on a logarithmic scale by curves 1 and 2 (left panel). For convenience, an artificial bias of 1 m was introduced into the phase path excesses. The phase path excesses L1 and L2 change from 2–5 m at 110-km height to 1,000 m at 1-km height. Curve 3 describes the altitude dependence of the contribution of the neutral atmosphere, isolated from the ionospheric impact by use of linear combination of the phase path excesses L1 and L2. This neutral atmosphere phase path excess changes over a broad dynamic range from 1 mm at 75 km to 1 km near the earth's surface. In contrast, the refractive attenuation X_a changes in a steep dynamic range from 0.05 to 1.1 over the height range 4–110 km (curve 1, right panel). Despite this difference, the relationship (6) brings to light an intrinsic connection between the phase path excess and intensity of RO signal. This may be seen from the comparison of the refractive attenuations X_a and X_p computed from the amplitude and phase data (right panel, curves 1 and 2). In order to convert the phase data according to Eq. 6, the phase acceleration a has been estimated numerically as the second derivative of the phase path excess with respect to time t by the use of a fixed time interval value of $\Delta t = 0.42$ s for differentiation. As a result of differentiation, the high-frequency noise level increases. This effect is seen in Fig. 2 (right panel).

The relationship (6) widens the applicability domain of the RO method. In particular, the RO method can be applied for estimating the integral absorption of radio waves in the atmosphere. The vertical profiles of the integral absorption of radio waves in the atmosphere are shown in Fig. 3 for five CHAMP RO measurement sessions conducted on 20 November 2003. The sessions 0175 and 0131 correspond to polar and moderately high latitude areas in the southern hemisphere (panels a and c); session 0187 refers to an equatorial region (panel b). Two sessions, 0096 and 0056, were carried out in areas of moderately high and polar latitude in the northern hemisphere (panels d and e). Therefore, these measurements represent conditions of radio wave propagation in all typical regions of the earth. The refractive attenuations, $X_a(t)$ and $X_p(t)$, recalculated from the amplitude and phase data using Eqs. 10 and 12 are shown on the left panels (curves 1 and 2). The smooth curves 3 indicate dependence of the refractive attenuation corresponding to the exponential altitude profile of the refractivity in the atmosphere with accounting for the total path absorption effect calculated by using the theoretical and experimental results reported by Kislyakov and Stankevich (1967) for decimeter-range radio waves. Excellent correspondence is seen between the refractive attenuations, $X_a(t)$ and $X_p(t)$, changing from 0 db at 40 km to −10 and −15 db at 5 km. There exists also a good correlation between the high-frequency part of variations in $X_a(t)$ and $X_p(t)$. However in Fig. 3 (left panels, c and e), good correspondence between the

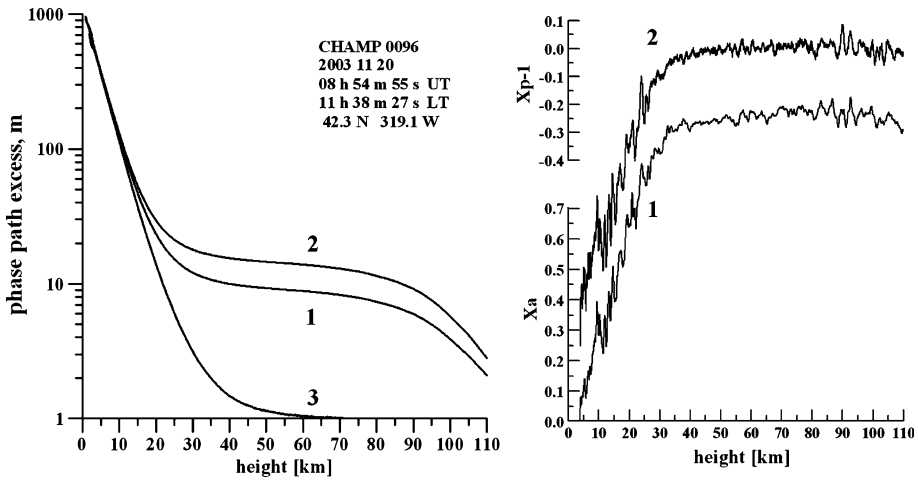

Fig. 2 Phase path excesses and attenuation at GPS frequencies L1 and L2 (curves 1 and 2). Curve 3 (left panel) corresponds to the contribution of the neutral atmosphere. The right panel shows the refractive attenuations X_a and X_p computed from the amplitude and phase data

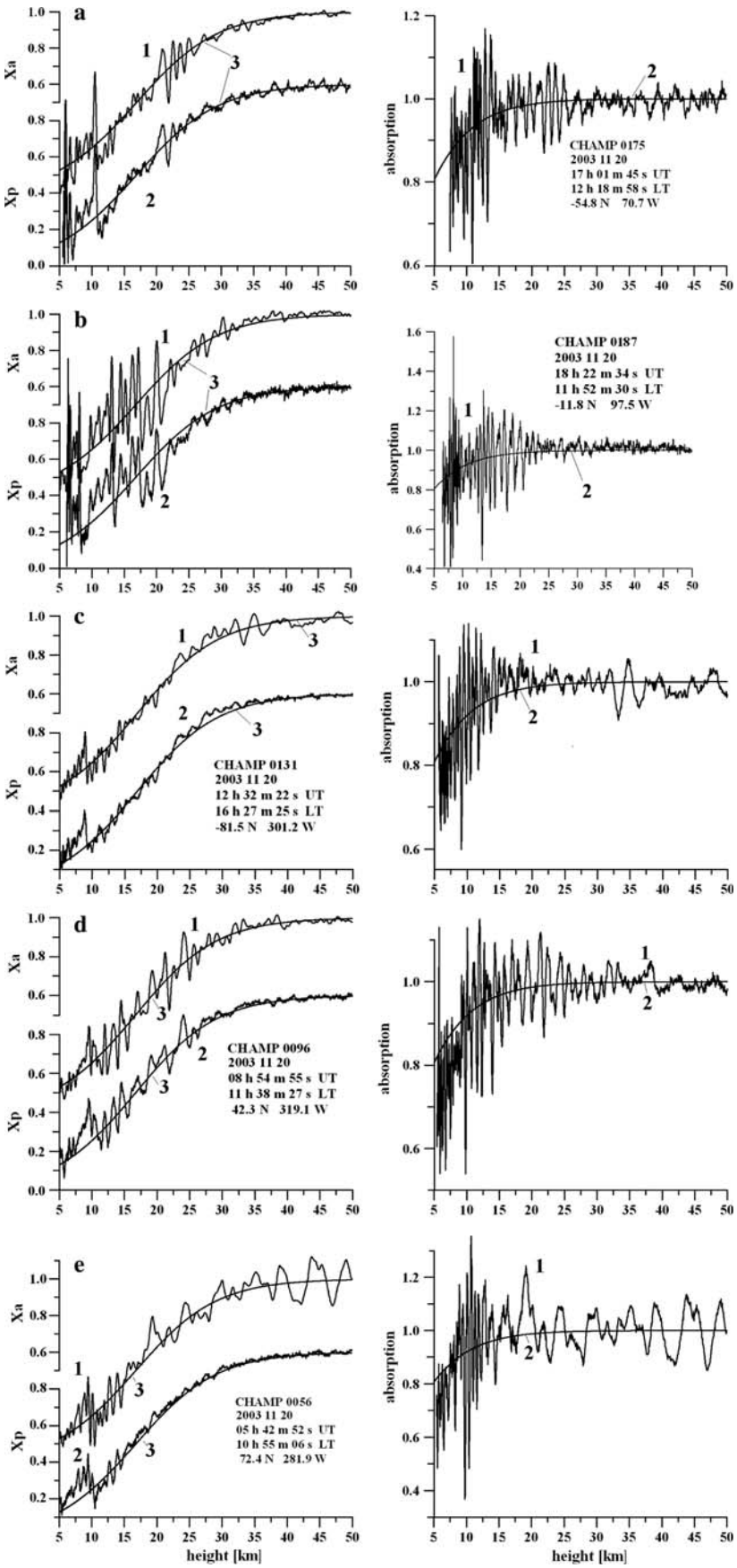

Fig. 3 Refractive attenuations at L1 GPS frequency and absorption. The *left panels* show the refractive attenuations $X_p(t)$ and $X_a(t)$ (curves 1 and 2). The smooth curves 3 indicate the dependence of the refractive attenuations accounting for the integral absorption in the atmosphere. The *right panels* show the integral absorption in the atmosphere

high-frequency part of variations in $X_a(t)$ and $X_p(t)$ exists only over an interval of 5–20 km. Above 20 km, the high-frequency variations of the refractive attenuation $X_a(t)$ are significantly greater than those of $X_p(t)$. This may be connected with the possible effect of transmitter–receiver instability and/or with ionospheric variability. The most probable cause is the influence of the polar ionospheric plasma structures that originated due to the impact of the intense geomagnetic storm, which occurred on 20 November 2003. The magnitude of the scintillation index S_4 equaled 13.7 and 7.4% in the polar measurement sessions, 0131 and 0056. The magnitude of the scintillation index S_4 was 5.5 and 4.2% (middle latitudes, sessions 0096 and 0175, left panels, a and d), and 4.8% in the equatorial area (session 0187, left panel, b). These values for the scintillation index S_4 are higher than those for quiet ionospheric conditions when S_4 changes mainly between 1 and 2% due to influence of the receiver noise. Therefore, the geomagnetic storm introduced significant contribution to the amplitude and phase variations of the RO signal, which is clearly seen in the polar regions of the earth. A more careful analysis of the ionospheric influence on the GPS RO signals is the subject of future investigation.

The apparent connection between the refractive attenuations restored from the amplitude and phase variations is useful for estimating the altitude dependence of the integral absorption in the atmosphere. This dependence is demonstrated by the rough curves 1 in Fig. 3 (right panels). The smooth curves 2 correspond to the integral absorption due to atmospheric oxygen calculated according to techniques described by Kislyakov and Stankevich (1967) and Yakovlev et al. (1995). Theoretically, the influence of the atmospheric oxygen is noticeable below 15–20 km. Experimental data support this theoretical suggestion. Below the altitude 8 km, the experimental data indicate additional attenuation compared with theoretical dependence. This may be connected with multipath propagation. Also, the influence of additional absorption in clouds and water vapor may be important below 8 km. Statistical analysis of this problem is in progress.

The preliminary results revealed good correspondence with theoretical values of attenuation described by Kislyakov and Stankevich (1967) and Yakovlev et al. (1995). The magnitude of the atmospheric absorption as measured at wavelength 32 cm (Pavelyev et al. 1996, 1997), which was estimated as 0.0096 ± 0.0024 dB km, coincides with experimental values of the integral attenuation indicated in Fig. 3 (right panels). It follows from our analysis that the refractive attenuations restored from the amplitude and phase variations are useful for estimating the integral absorption, recognizing layered structures in the atmosphere and revealing the systematic errors in the amplitude data.

Location of layered structures

Using Eqs. 6–9 the distance $\mathrm{LT} \approx \mathrm{LD} = d_{2s}(T)$ from simultaneous observation of the phase and intensity variations may be found,

$$d_{2s}(T) = 2R_0\beta\left[1 + 2\beta(1 - v/w) + (1 - 4\beta\, v/w)^{1/2}\right]^{-1} \tag{13}$$

with $\beta = mw^2/R_0$; m is introduced in Eqs. 6 and 7. If parameter m is estimated from the experimental data, it is possible to find the new value of distance $\mathrm{LT}' \equiv d_{2s}(T')$ and thus determine the displacement $d = TT'$ of the new tangent point T' relative to the point T (Fig. 1). We assume that m is a slowly changing function of time. If the receiver noise is small, averaging is not necessary and m can be determined directly from Eq. 6 as a ratio

$$m = [1 - X(t)]/a \tag{14}$$

In the presence of noise, the value $m(t_k)$ corresponding to some instant of time t_k can be determined in two ways, from a correlation relationship

$$m(t_k) = \sum_{i=k-M}^{k+M} [X(t_i) - 1]a(t_i) \Bigg/ \sum_{i=k-M}^{k+M} [a(t_i)]^2 \tag{15}$$

or from the ratio of the time averages of the squared values of the refractive attenuation and phase acceleration,

$$m(t_k) = \left\{ \sum_{i=k-M}^{k+M} [X(t_i) - 1]^2 \Bigg/ \sum_{i=k-M}^{k+M} [a(t_i)]^2 \right\}^{1/2} \tag{16}$$

where $2M + 1$ is a number of samples for averaging, and $X(t_i)$ and $a(t_i)$ are the refractive attenuation and phase acceleration variations, respectively, at the time instant t_i. Eqs. 15 and 16 give different estimates for the parameter m. Then, by using Eq. 13, one can estimate the displacement $d = d_{2s}(T') - d_{2s}(T) \approx d_{2s}(T') - (R_2^2 - p^2)^{1/2}$. In the case of full correlation between the refractive attenuation and phase acceleration, the influence of the layered structures prevails and the magnitudes of parameter m and displacement d can be evaluated exactly.

Examples of the suggested method are given below using an analysis of FORMOSAT3 RO measurements. Descriptions of the FORMOSAT3 mission are found in Liou et al. (2007) and Fong et al. (2008a). Its first-year performance and achievement is given in Fong et al. (2008b). An example of determination of the displacement d is shown in Fig. 4. The data shown correspond to the FORMOSAT3 RO session 0035 conducted on 24 April 2006, 16 h 04 m LT, with geographical coordinates 17.5°S and 235.7°W. Curves 1 and 2 (left panel) demonstrate significant similarities between the refractive attenuations X_a and X_p evaluated from the phase acceleration and

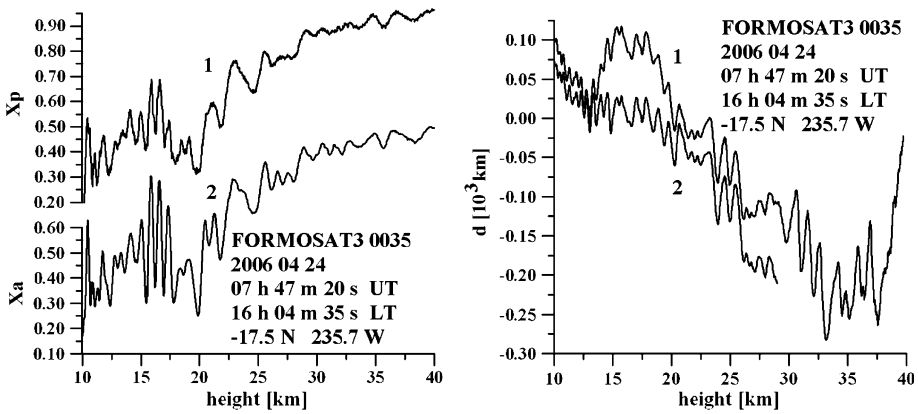

Fig. 4 Refractive attenuation and displacement d of the tangent point T. The displacements were calculated with Eqs. 15 and 16 (curves 1 and 2, respectively)

amplitude data at the GPS L1 frequency. This coincidence allows one to determine the horizontal displacement d of the tangent point T. The results of evaluating the displacement d with Eqs. 13, 15 and 16 are shown in the right panel. Curves 1 and 2 correspond to values d found using relationships (13), (15) and (13), (16), respectively. The estimated displacement d is bounded between ±50 km for the height range 10–20 and ±100 km over the height range 20–40 km. This indicates a possible applicability of the RO method for location of the layered structures in the atmosphere.

Figure 5 demonstrates two application examples of the phase acceleration technique to investigate plasma layers in the lower ionosphere provided by analysis of FORMOSAT-3 RO data. The measurements were obtained during sessions 0047 and 0087 on 25 and 29 April 2006, respectively. The left panels show curves 1 and 2 corresponding to the refractive attenuations X_a and X_p, respectively. Also the left panels show curves 3 indicating the results of determining the deflection d of point T. The deflection d was estimated from Eqs. 13 and 15 by averaging over a time interval equal to 1.5 s. The distance d changes between 600–800 km and 280–510 km with statistical error ±110 and ±70 km, respectively. The average value of distance d is 590 and 350 km, respectively. Using these values it is possible to find the actual height $h'(T')$ and the inclination δ of the investigated plasma layers (Wickert et al. 2004) as

$$h'(T') = h + d^2/2r_0 \quad (17)$$

$$\delta = d/r_0 \quad (18)$$

where r_0 is the earth radius, and h is the height of the ray perigee T. For the RO data shown in Fig. 5 (left panels), the real height of the sporadic E_s layers is greater than the height of the ray perigee h by 11.8 km and 30.0 km, respectively, with an average layer inclination δ of about 2.5°–5°. The positive values d correspond to the displacement along the ray GTL from the ray perigee T to the GPS satellite.

After estimation of the average height and distance d, one has to apply the method for solving the inverse problem described in Liou et al. (2005). In accordance with this method, the vertical gradient of the refractivity and the altitude profile of the electron density are retrieved based on variations in the RO signal amplitude. Then, after integration, the vertical profile of electron density variations $\delta Ne(h')$ is found. The results of retrieving the variations $\delta Ne(h')$ in the electron density and its gradient $d\delta Ne(h')/dh'$ are shown in Fig. 5 for sessions 0047 and 0087 (right panels, a and b). Variations in the refractive attenuations X_a and X_p are shown by curves 1 and 2. Curves 3 and 4 describe the retrieved variations, $\delta Ne(h')$ and $d\delta Ne(h')/dh'$, by means of Eq. 17 as functions of the adjusted altitude h'. Curves 1 and 2 agree well. Actually, it is another example of the validity of Eq. 6 for the case of the sporadic E_s layer. According to the right panels, the perturbations $\delta Ne(h')$ of the electron density lie within the range $\pm 14 \cdot 10^9$ el/m^3 (session 0047) and $\pm 36 \cdot 10^9$ el/m^3 (session 0087). The vertical gradient $d\delta Ne(h')/dh'$ changes over $\pm 12 \cdot 10^9$ el/m^3/km (session 0047) and $\pm 41 \cdot 10^9$ el/m^3/km (session 0087). The increased values in electron density and vertical gradient for session 0087 are related to the increased variation in the refractive attenuation by a factor of about three (left panels, a, b, curves 1 and 2). These variations correspond to the typical values in the sporadic E_s layers in the altitude range 90–130 km (Igarashi et al. 2002; Wu Dong et al. 2005; Kelly 1989). Although the analysis provided is preliminary, it indicates a possibility of establishing in some cases the actual location, height and inclination of sporadic E_s structures in the ionosphere from a single RO vertical profile. Analysis of the practical importance of this method for remote sensing of sporadic plasma layers in the ionosphere is in progress.

Conclusion

An important connection between the phase acceleration, Doppler frequency and intensity variations of RO signal

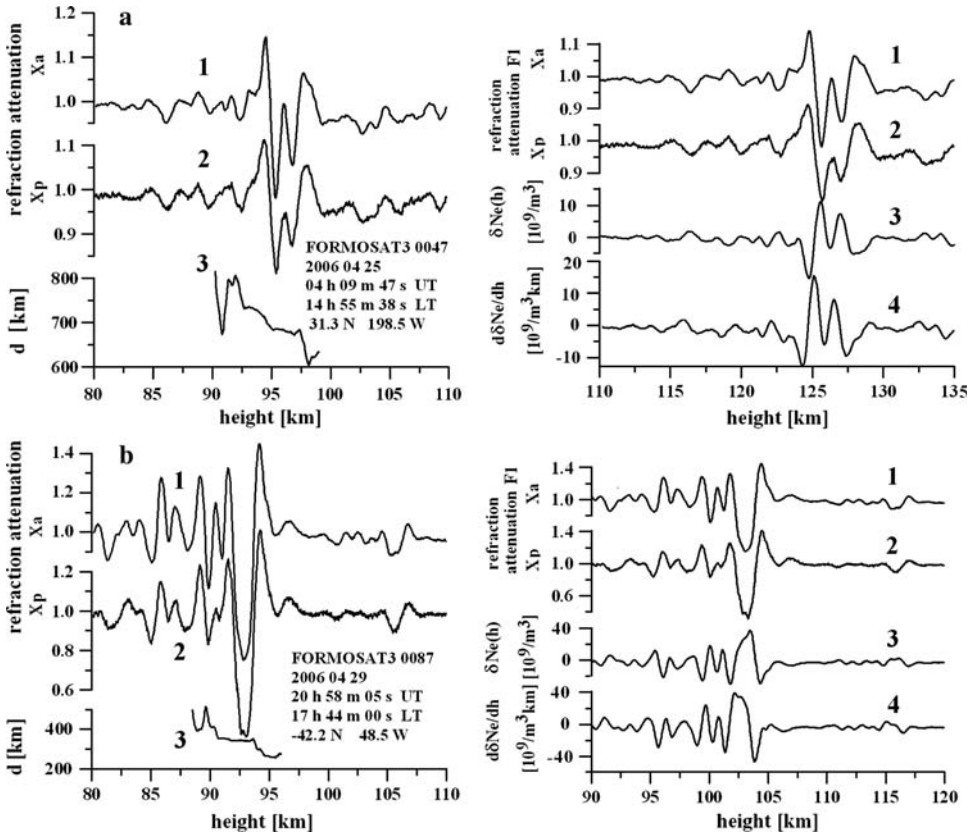

Fig. 5 Results of the 25 and 29 April 2006 occultation sessions. The left panels show the refractive attenuations X_a and X_p evaluated from the amplitude and phase data and the estimated distance d obtained from combined analysis of phase and amplitude variations. The right panels show refractive attenuations (curves 1 and 2), retrieved variations of the electron density and its vertical gradient (curves 3 and 4) as functions of the height of sporadic E_s layer

was described in theory and validated by experimental analysis with radio-holograms registered during CHAMP and FORMOSAT-3 missions (Liou and Pavelyev 2006; Pavelyev et al. 2007). The discovered connection gives a possibility to convert the phase acceleration (or time derivative of Doppler frequency) into refractive attenuation. This is useful for estimating the integral absorption of radio waves in trans-atmospheric communication links. Such estimations are relevant for measuring water vapor and minor atmospheric gas constituents in future RO missions, because the difficulty of removing the refractive attenuation effect from the amplitude data can be avoided. The new method, based on the combined analysis of variations in the phase acceleration and the refractive attenuation, is promising for the localization of layered structures in the near-earth space. A possibility for application of this method is illustrated by the analysis of the RO experimental data recorded by the CHAMP and FORMOSAT-3 satellites. The application of this and other new techniques will generate a more extensive body of information on plasma structures and natural processes in the ionosphere and their connection with processes in magnetosphere and interplanetary space.

Acknowledgments We are grateful to NSPO (Taiwan) and UCAR (USA) for making FORMOSAT3 experimental RO data available. This work was jointly supported by the Russian Foundation for Basic Research, project no. 06-02-17071, the National Science Council of Taiwan, grant no. NSC 96-2811-M-008-061, and the NSPO (Taiwan), grant no. 97-NSPO(B)-SP-FA07-03(F).

References

Fong CJ, Shiau WT, Lin CT, Kuo TC, Chu CH, Yang SK, Yen N, Chen SS, Kuo YH, Liou YA, Chi S (2008a) Constellation deployment for FORMOSAT-3/COSMIC mission. IEEE Trans Geosci Remote Sens 46(11):3367–3379. doi:10.1109/TGRS.2008.2005202

Fong CJ, Yang S-K, Chu CH, Huang CY, Yeh JJ, Lin CT, Kuo TC, Liu TY, Yen N, Chen SS, Kuo YH, Liou YA, Chi S (2008b) FORMOSAT-3/COSMIC constellation spacecraft system performance: after one year in orbit. IEEE Trans Geosci Remote Sens 46(11):3380–3394. doi:10.1109/TGRS.2008.2005203

Gorbunov ME, Bengtson L (1996) Advanced algorithms of inversion of GPS/MET satellite data and their application to reconstruction of temperature and humidity. Tech. Rep Report No. 211, Max Planck Institute for Meteorology, Hamburg

Gorbunov ME, Lauritsen KB (2002) Canonical transform methods for radio occultation data. Scientific Report 02-10 Danish Meteorological Institute, Copenhagen

Gorbunov ME, Gurvich AS, Shmakov AV (2002) Back-propagation and radio-holographic methods for investigation of sporadic ionospheric E-layers from Microlab-1 data. Int J Remote Sens 23(4):675–685. doi:10.1080/01431160010030091

Gurvich AS, Krasil'nikova TG (1987) Radio occultation investigation of the atmosphere with usage GPS satellites. Cosm Res 25(6):89–95

Hajj GA, Kursinski ER, Romans LJ et al (2002) Technical description of atmospheric sounding by GPS occultation. J Atmos Sol Terr Phys 64:451–469. doi:10.1016/S1364-6826(01)00114-6

Hinson DP, Flasar FM, Schinder A, Twicken JD, Herrera RG (1997) Jupiter's ionosphere: results from the first Galileo radio occultation experiment. Geophys Res Lett 24(18):2107–2110. doi:10.1029/97GL01608

Hocke KA, Pavelyev AG, Yakovlev OI, Barthes L, Jakowski N (1999) Radio occultation data analysis by the radioholographic method. J Atmos Sol Terr Phys 61(16):1169–1178. doi:10.1016/S1364-6826(99)00080-2

Igarashi K, Pavelyev AG, Hocke K, Kucherjavenkov A, Matugov S, Yakovlev O, Pavelyev D, Zakharov A (2000) Radio holographic principle for observing natural processes in the atmosphere and retrieving meteorological parameters from radio occultation data. Earth Planets Space 52(11):868–875

Igarashi K, Pavelyev A, Hocke K, Pavelyev D, Wickert J (2001) Observation of wave structures in the upper atmosphere by means of radio holographic analysis of the radio occultation data. Adv Space Res 27(6–7):1321–1327

Igarashi K, Pavelyev A, Wickert J, Hocke K, Pavelyev D (2002) Application of radio holographic method for observation of altitude variations of the electron density in the mesosphere/lower thermosphere using GPS/MET radio occultation data. J Atmos Sol Terr Phys 64(4):959–969. doi:10.1016/S1364-6826(02)00050-0

Jensen AS, Lohmann M, Benzon HH, Nielsen AS (2003) Full spectrum inversion of radio occultation signals. Radio Sci 38(3):1040. doi:10.1029/2002RS002763

Kalashnikov IE, Matyugov SS, Pavelyev AG, Yakovlev OI (1986) Electromagnetic waves in the atmosphere and space. Nauka, Moscow, pp 208–218 (in Russian)

Kelly MC (1989) The Earth's Ionosphere. Int. Geophys. Ser. 43 Elsevier, New York

Kislyakov AG, Stankevich KS (1967). Absorption of Radio Waves in the Atmosphere Izv Vyssh Uchebn Zaved Radiophyz 10(9–10): 1244–1270 (in Russian)

Kursinski ER, Hajj GA, Schofield JT, Linfield RP, Hardy KR (1997) Observing the Earth's atmosphere with radio occultation measurements using the Global Positioning System. J Geophys Res 102:23,429–23,465. doi:10.1029/97JD01569

Lindal GF, Lyons JR, Sweetnam DN, Eshleman VR, Hinson DP, Tyler GL (1987) The atmosphere of Uranus: Results of radio occultation measurements with Voyager 2. J Geophys Res 92(A13):14,987–15,001. doi:10.1029/JA092iA13p14987

Liou YA, Pavelyev AG, Wickert J, Schmidt T, Pavelyev AA (2005) Analysis of atmospheric and ionospheric structures using the GPS/MET and CHAMP radio occultation database: a methodological review. GPS Solut 9:122–143. doi:10.1007/s10291-005-0141-y

Liou YA, Pavelyev AG, Liu SF, Pavelyev AA, Yen N, Huang CY, Fong CJ (2007) FORMOSAT-3 GPS radio occultation mission: preliminary results. IEEE Trans Geosci Remote Sens 45(10): 3813–3826. doi:10.1109/TGRS.2007.903365

Liu AS (1978) On the determination and investigation of the terrestrial ionospheric refractive indices using GEOS-3/ATS-6 satellite-to-satellite tracking data. Radio Sci 13(4):709–716. doi:10.1029/RS013i004p00709

Liou YA, Pavelyev, AG (2006) Simultaneous observations of radio wave phase and intensity variations for locating the plasma layers in the ionosphere. Geophys Res Lett 33(23):L23102 1–5

Lohman MS, Jensen AS, Benson HH, Nielsen AS (2003) Radio occultation retrieval of atmospheric absorption based on FSI. Report 03-22 Danish Meteorological Institute, Copenhagen

Marouf EA, Tyler GL, Rosen PA (1986) Profiling Saturn rings by radio occultation. Icarus 68:120–166. doi:10.1016/0019-1035(86)90078-3

Melbourne WG (2004) Radio occultations using Earth satellites: a wave theory treatment. Jet Propulsion Laboratory California Institute of Technology, Monograph 6 Deep space communications and navigation series

Mortensen MD, Hoeg P (1998) Inversion of GPS occultation measurements using Fresnel diffraction theory. Geophys Res Lett 25(14):2446–2449

Pavelyev AG (1998) On the feasibility of radioholographic investigations of wave fields near the Earth's radioshadow zone on the satellite-to-satellite path. J Commun Technol Electron 43(8):875–879

Pavelyev AG, Volkov AV, Zakharov AI, Krutikh SA, Kucherjavenkov AI (1996) Bistatic radar as a tool for earth investigation using small satellites. Acta Astronaut 39(9–12):721–730. doi:10.1016/S0094-5765(97)00055-6

Pavelyev AG, Zakharov AI, Kucheryavenkov AI, Molotov EP, Sidorenko AI, Kucheryavenkova IL, Pavelyev DA (1997) Propagation of radio waves reflected from Earth's surface at grazing angles between a low-orbit space station and a geostationary satellite. J Commun Technol Electron 42(1):51–57

Pavelyev AG, Igarashi K, Reigber C, Hocke K, Wickert J, Beyerle G, Matyugov S, Kucherjavenkov A, Pavelyev D, Yakovlev OI (2002) First application of the radio holographic method to wave observations in the upper atmosphere. Radio Sci 37(3):15-1–15-11

Pavelyev AG, Liou YA, Wickert J (2004) Diffractive vector and scalar integrals for bistatic radio-holographic remote sensing. Radio Sci 39(4):RS4011 1–16

Pavelyev AG, Liou YA, Wickert J, Schmidt T, Pavelyev AA, Liu SF (2007) Effects of the ionosphere and solar activity on radio occultation signals: application to Challenging Minisatellite Payload satellite observations. J Geophys Res 112(A06326):1–14. doi:10.1029/2006JA011625

Rangaswamy S (1976) Recovery of Atmospheric Parameters from the Apollo/Soyuz-ATS-F Radio Occultation Data. Geophys Res Lett 3(8):483–486. doi:10.1029/GL003i008p00483

Rocken C, Anthes R, Exner M et al (1997) Analysis and validation of GPS/MET data in the neutral atmosphere. J Geophys Res 102:29849–29866. doi:10.1029/97JD02400

Sokolovskiy SV (2001) Modeling and inverting radio occultation signals in the moist troposphere. Radio Sci 36(3):441–458. doi:10.1029/1999RS002273

Sokolovskiy SV, Schreiner W, Rocken C, Hunt D (2002) Detection of high-altitude ionospheric irregularities with GPS/MET. Geophys Res Lett 29(3):1033–1037. doi:10.1029/2001GL013398

Ware R, Exner M, Feng D, Gorbunov M et al (1996) GPS sounding of the atmosphere from low Earth orbit: preliminary results. Bull Am Meteorol Soc 77(1):19–40. doi:10.1175/1520-0477(1996)077<0019:GSOTAF>2.0.CO;2

Wickert J, Pavelyev AG, Liou YA, Schmidt T, Reigber Ch, Igarashi K, Pavelyev AA, Matyugov SS (2004) Amplitude scintillations in GPS signals as a possible indicator of ionospheric structures. Geophys Res Lett 31(24):L24801 1–4

Wu Dong L, Ao Chi O, Hajj GA, Manuel de la Torre Juarez, Mannucci AJ (2005) Sporadic E morphology from GPS-CHAMP radio occultation. J Geoph Res 110: A01306 1–18

Yakovlev OI (2003) Space Radio Science. Taylor and Francis, London

Yakovlev OI, Matyugov SS, Vilkov IA (1995) Attenuation and scintillation of radio waves in the Earth's atmosphere in radio occultation experiments on the satellite-to-satellite link. Radio Sci 30:591–600. doi:10.1029/94RS01920

Yunck T, Lindal G, Liu CH (1988) The role of GPS in precise Earth observations. Proceedings of the IEEE Position Location and Navigation Symposium. Orlando, Florida